

DANYELLE ANDRADE MOTA
(Organizadora)

ENGENHARIAS:

Criação e repasse de tecnologias 3



DANYELLE ANDRADE MOTA
(Organizadora)

ENGENHARIAS:

Criação e repasse de tecnologias 3



Editora chefe

Profª Drª Antonella Carvalho de Oliveira

Editora executiva

Natalia Oliveira

Assistente editorial

Flávia Roberta Barão

Bibliotecária

Janaina Ramos

Projeto gráfico

Bruno Oliveira

Camila Alves de Cremo

Daphynny Pamplona

Luiza Alves Batista

Natália Sandrini de Azevedo

Imagens da capa

iStock

Edição de arte

Luiza Alves Batista

2022 by Atena Editora

Copyright © Atena Editora

Copyright do texto © 2022 Os autores

Copyright da edição © 2022 Atena Editora

Direitos para esta edição cedidos à Atena Editora pelos autores.

Open access publication by Atena Editora



Todo o conteúdo deste livro está licenciado sob uma Licença de Atribuição *Creative Commons*. Atribuição-Não-Comercial-Não-Derivativos 4.0 Internacional (CC BY-NC-ND 4.0).

O conteúdo dos artigos e seus dados em sua forma, correção e confiabilidade são de responsabilidade exclusiva dos autores, inclusive não representam necessariamente a posição oficial da Atena Editora. Permitido o *download* da obra e o compartilhamento desde que sejam atribuídos créditos aos autores, mas sem a possibilidade de alterá-la de nenhuma forma ou utilizá-la para fins comerciais.

Todos os manuscritos foram previamente submetidos à avaliação cega pelos pares, membros do Conselho Editorial desta Editora, tendo sido aprovados para a publicação com base em critérios de neutralidade e imparcialidade acadêmica.

A Atena Editora é comprometida em garantir a integridade editorial em todas as etapas do processo de publicação, evitando plágio, dados ou resultados fraudulentos e impedindo que interesses financeiros comprometam os padrões éticos da publicação. Situações suspeitas de má conduta científica serão investigadas sob o mais alto padrão de rigor acadêmico e ético.

Conselho Editorial**Ciências Exatas e da Terra e Engenharias**

Prof. Dr. Adélio Alcino Sampaio Castro Machado – Universidade do Porto

Profª Drª Alana Maria Cerqueira de Oliveira – Instituto Federal do Acre

Profª Drª Ana Grasielle Dionísio Corrêa – Universidade Presbiteriana Mackenzie

Profª Drª Ana Paula Florêncio Aires – Universidade de Trás-os-Montes e Alto Douro

Prof. Dr. Carlos Eduardo Sanches de Andrade – Universidade Federal de Goiás

Profª Drª Carmen Lúcia Voigt – Universidade Norte do Paraná



Prof. Dr. Cleiseano Emanuel da Silva Paniagua – Instituto Federal de Educação, Ciência e Tecnologia de Goiás
Prof. Dr. Douglas Gonçalves da Silva – Universidade Estadual do Sudoeste da Bahia
Prof. Dr. Eloi Rufato Junior – Universidade Tecnológica Federal do Paraná
Profª Drª Érica de Melo Azevedo – Instituto Federal do Rio de Janeiro
Prof. Dr. Fabrício Menezes Ramos – Instituto Federal do Pará
Profª Dra. Jéssica Verger Nardeli – Universidade Estadual Paulista Júlio de Mesquita Filho
Prof. Dr. Juliano Bitencourt Campos – Universidade do Extremo Sul Catarinense
Prof. Dr. Juliano Carlo Rufino de Freitas – Universidade Federal de Campina Grande
Profª Drª Luciana do Nascimento Mendes – Instituto Federal de Educação, Ciência e Tecnologia do Rio Grande do Norte
Prof. Dr. Marcelo Marques – Universidade Estadual de Maringá
Prof. Dr. Marco Aurélio Kistemann Junior – Universidade Federal de Juiz de Fora
Prof. Dr. Miguel Adriano Inácio – Instituto Nacional de Pesquisas Espaciais
Profª Drª Neiva Maria de Almeida – Universidade Federal da Paraíba
Profª Drª Natiéli Piovesan – Instituto Federal do Rio Grande do Norte
Profª Drª Priscila Tessmer Scaglioni – Universidade Federal de Pelotas
Prof. Dr. Sidney Gonçalo de Lima – Universidade Federal do Piauí
Prof. Dr. Takeshy Tachizawa – Faculdade de Campo Limpo Paulista



Engenharias: criação e repasse de tecnologias 3

Diagramação: Camila Alves de Cremona
Correção: Maiara Ferreira
Indexação: Amanda Kelly da Costa Veiga
Revisão: Os autores
Organizadora: Danyelle Andrade Mota

Dados Internacionais de Catalogação na Publicação (CIP)

E57 Engenharia: criação e repasse de tecnologias 3 /
Organizadora Danyelle Andrade Mota. – Ponta Grossa -
PR: Atena, 2022.

Formato: PDF

Requisitos de sistema: Adobe Acrobat Reader

Modo de acesso: World Wide Web

Inclui bibliografia

ISBN 978-65-258-0506-1

DOI: <https://doi.org/10.22533/at.ed.061220509>

1. Engenharia. 2. Tecnologia. I. Mota, Danyelle Andrade
(Organizadora). II. Título.

CDD 620

Elaborado por Bibliotecária Janaina Ramos – CRB-8/9166

Atena Editora
Ponta Grossa – Paraná – Brasil
Telefone: +55 (42) 3323-5493
www.atenaeditora.com.br
contato@atenaeditora.com.br



Atena
Editora
Ano 2022

DECLARAÇÃO DOS AUTORES

Os autores desta obra: 1. Atestam não possuir qualquer interesse comercial que constitua um conflito de interesses em relação ao artigo científico publicado; 2. Declaram que participaram ativamente da construção dos respectivos manuscritos, preferencialmente na: a) Concepção do estudo, e/ou aquisição de dados, e/ou análise e interpretação de dados; b) Elaboração do artigo ou revisão com vistas a tornar o material intelectualmente relevante; c) Aprovação final do manuscrito para submissão.; 3. Certificam que os artigos científicos publicados estão completamente isentos de dados e/ou resultados fraudulentos; 4. Confirmam a citação e a referência correta de todos os dados e de interpretações de dados de outras pesquisas; 5. Reconhecem terem informado todas as fontes de financiamento recebidas para a consecução da pesquisa; 6. Autorizam a edição da obra, que incluem os registros de ficha catalográfica, ISBN, DOI e demais indexadores, projeto visual e criação de capa, diagramação de miolo, assim como lançamento e divulgação da mesma conforme critérios da Atena Editora.



DECLARAÇÃO DA EDITORA

A Atena Editora declara, para os devidos fins de direito, que: 1. A presente publicação constitui apenas transferência temporária dos direitos autorais, direito sobre a publicação, inclusive não constitui responsabilidade solidária na criação dos manuscritos publicados, nos termos previstos na Lei sobre direitos autorais (Lei 9610/98), no art. 184 do Código Penal e no art. 927 do Código Civil; 2. Autoriza e incentiva os autores a assinarem contratos com repositórios institucionais, com fins exclusivos de divulgação da obra, desde que com o devido reconhecimento de autoria e edição e sem qualquer finalidade comercial; 3. Todos os e-book são *open access*, *desta forma* não os comercializa em seu site, sites parceiros, plataformas de *e-commerce*, ou qualquer outro meio virtual ou físico, portanto, está isenta de repasses de direitos autorais aos autores; 4. Todos os membros do conselho editorial são doutores e vinculados a instituições de ensino superior públicas, conforme recomendação da CAPES para obtenção do Qualis livro; 5. Não cede, comercializa ou autoriza a utilização dos nomes e e-mails dos autores, bem como nenhum outro dado dos mesmos, para qualquer finalidade que não o escopo da divulgação desta obra.



APRESENTAÇÃO

A engenharia é uma ciência que utiliza de conhecimentos e estudos técnicos e científicos com o intuito de criar e otimizar novas ferramentas, métodos, processos, desenvolver novas tecnologias, corrigir falhas nos procedimentos ou produtos. Sua abrangência envolve todas as áreas de atuação humana, e é um dos pilares do desenvolvimento tecnológico, social e econômico da sociedade.

Pode-se dizer que a engenharia é um sinônimo de desenvolvimento e um dos principais pilares para o setor industrial. Logo, entender os campos de atuação, bem como pontos de inserção e melhoria dessa desta área é de grande importância, buscando desenvolver novos métodos e ferramentas para melhoria continua de processos.

A coleção “ENGENHARIAS: CRIAÇÃO E REPASSE DE TECNOLOGIAS 3” é uma obra que tem como foco principal a discussão científica de forma interdisciplinar com trabalhos, pesquisas, relatos de casos e/ou revisões que transitam nos vários caminhos das Engenharias e áreas afins. O objetivo central foi apresentar de forma categorizada e clara estudos desenvolvidos em diversas instituições de ensino e pesquisa.

Na presente obra são apresentados 15 trabalhos teóricos e práticos, relacionados as áreas de engenharia, como civil, materiais, mecânica, química, ambiental, dentre outras, dando um viés onde se faz necessária a melhoria continua em processos, projetos e na gestão geral no setor fabril e empreendedor. Destaca-se ainda a busca da redução de custos, sustentabilidade, melhoria continua e otimização de processos.

De abordagem objetiva, a obra se mostra de grande relevância para graduandos, alunos de pós-graduação, docentes e profissionais, apresentando temáticas e metodologias diversificadas, em situações reais. Sendo hoje que utilizar dos conhecimentos científicos de uma maneira eficaz e eficiente é um dos desafios dos novos engenheiros. Agradeço aos autores pelas contribuições que tornaram essa edição possível, e juntos, convidamos os leitores para desfrutarem as publicações.

Tenham uma ótima leitura!

Danyelle Andrade Mota

SUMÁRIO

CAPÍTULO 1..... 1

A BIOMASSA COMO FONTE RENOVÁVEL DE ENERGIA ELÉTRICA: UMA REVISÃO CONTEXTUAL


Brenda Leal Mota Santos
Renato Santos Freire Ferraz
Patrick Laurient Cardoso Silva
Fábio Vincenzi Romualdo da Silva
Adjeferson Custódio Gomes
Rafael Rodrigues de Queiroz Freitas

 <https://doi.org/10.22533/at.ed.0612205091>

CAPÍTULO 2..... 13

REMOÇÃO DE COR E TOXICIDADE DE EFLUENTE TÊXTIL A PARTIR DE CIANOBACTÉRIAS


Sílvia Mariana da Silva Barbosa
Marcella Vianna Cabral Paiva

 <https://doi.org/10.22533/at.ed.0612205092>

CAPÍTULO 3..... 21

A APLICAÇÃO DE *ANALYTIC NETWORK PROCESS* - ANP EM LOGÍSTICA REVERSA: UMA ANÁLISE BIBLIOMÉTRICA


Jovani Patias
Leoni Pentiado Godoy
Murilo Sagrillo Pereira
Bruno Miranda dos Santos
Cyro Rei Prato Neto

 <https://doi.org/10.22533/at.ed.0612205093>

CAPÍTULO 4..... 34

UMA AVALIAÇÃO DOS INDICADORES DE PERDA DE ÁGUA NUM PERÍODO DE ESCASSEZ HÍDRICA NO MUNICÍPIO DE VITÓRIA NO ESTADO DO ESPÍRITO SANTO


Diênifer Calegari Leopoldino Guimarães






 <https://doi.org/10.22533/at.ed.0612205094>


CAPÍTULO 5..... 51

DESENVOLVIMENTO DE SURFACTANTE COM VISCOSIDADE ADAPTÁVEL PARA AUMENTAR A EXTRAÇÃO DE ÓLEO NA RECUPERAÇÃO AVANÇADA DE PETRÓLEO

Laura Procópio Maia Furbino
Edilailsa Januário de Melo
Rogério Alexandre Alves de Melo
José Izaquiel Santos da Silva

 <https://doi.org/10.22533/at.ed.0612205095>

CAPÍTULO 6	62
USO DE SENSOR PIEZOELÉTRICO NA DETERMINAÇÃO DO ATRASO DE IGNIÇÃO EM UM MOTOR DE COMBUSTÃO DO CICLO DIESEL	
Márcio Andrade Rocha Lesso Benedito dos Santos Carlos A. Cabral Santos Jefferson W. de M. Mendonça	
 https://doi.org/10.22533/at.ed.0612205096	
CAPÍTULO 7	68
APLICAÇÕES E LIMITAÇÕES DO GESSO NA CONSTRUÇÃO CIVIL	
Augusto Cury Braff	
 https://doi.org/10.22533/at.ed.0612205097	
CAPÍTULO 8	82
REVISÃO DOS MÉTODOS DE DIMENSIONAMENTO ESTRUTURAL DE VIGAS MISTAS CONCRETO/MADEIRA	
Guilherme Barbosa Vieira Thyago Camelo Pereira da Silva	
 https://doi.org/10.22533/at.ed.0612205098	
CAPÍTULO 9	105
DESENVOLVIMENTO DE TEAR PLANO MODULAR IMPRESSO EM 3D PARA PRODUÇÃO DE TECIDOS DE PEQUENA LARGURA	
Matheus da Silva Rodrigues Fabia Regina Gomes Ribeiro Daniel Perdigão Lobato Liliana de Luca Xavier Augusto Leandro da Silva Pereira	
 https://doi.org/10.22533/at.ed.0612205099	
CAPÍTULO 10	111
FATIGUE PROPERTIES OF COMBINED FRICTION STIR AND ADHESIVELY BONDED AA6082-T6 OVERLAP JOINTS	
Ricardo Maciel Tiago Bento Daniel F.O. Braga Lucas F.M. da Silva Pedro M.G.P. Moreira Virgínia Infante	
 https://doi.org/10.22533/at.ed.06122050910	
CAPÍTULO 11	128
MINIMIZAÇÃO DE DESLOCAMENTO DE OPERADORES POR MEIO DE AGRUPAMENTO DE FERRAMENTAIS EM ARRANJOS FÍSICOS POSICIONAIS	
Chin Yung Shih	

 <https://doi.org/10.22533/at.ed.06122050911>

CAPÍTULO 12..... 149

MÓDULO ELETRÔNICO SINTETIZADO SEM FIO, PARA BATERIA ELETRÔNICA, ATRAVÉS DA COMUNICAÇÃO WI-FI DO ESP32

Paulo César do Nascimento Cunha

Afonso Pereira Barros

Gabriel Vinícius de Souza Bispo

José Irineu Ferreira Júnior

Jarlisson José de Lira

 <https://doi.org/10.22533/at.ed.06122050912>

CAPÍTULO 13..... 158

APLICAÇÕES DO DESIGN INSTRUCIONAL NA DISCIPLINA DE DESENHO: MÉTODOS DE ENSINO CONTEXTUALIZADOS PARA O ENSINO MÉDIO

José Rodolfo Ribeiro Tavares

Giselle Aparecida de Sousa Araujo


Isabel Barros Fiaux dos Santos

Luciene Maria de Souza Zanardi

Maria Cecília da Silva Barbosa

Paulo Roberto Boldarini Regini

Yasmim Carolino Bora Marinho

 <https://doi.org/10.22533/at.ed.06122050913>

CAPÍTULO 14..... 173

QUESTÕES NORTEADORAS PARA ESTUDO DE USABILIDADE EM POLÍTICAS DE SEGURANÇA DA INFORMAÇÃO EM VSEs

André Rivas

Ivanir Costa

Nilson Salvetti

Marcos Vinícius da Silva Messias

Osmair Mendes Pereira

 <https://doi.org/10.22533/at.ed.06122050914>

CAPÍTULO 15..... 185

O EMPREENDEDORISMO FEMININO E SUAS PRINCIPAIS VERTENTES

Isadora dos Santos Raposo

Maurício Guerreiro

 <https://doi.org/10.22533/at.ed.06122050915>

SOBRE A ORGANIZADORA..... 190

ÍNDICE REMISSIVO..... 191

FATIGUE PROPERTIES OF COMBINED FRICTION STIR AND ADHESIVELY BONDED AA6082-T6 OVERLAP JOINTS

Data de aceite: 01/09/2022

Ricardo Maciel

LAETA, IDMEC, Instituto Superior Técnico,
Universidade de Lisboa
Portugal
<https://orcid.org/0000-0002-7920-000X>

Tiago Bento

LAETA, IDMEC, Instituto Superior Técnico,
Universidade de Lisboa
Portugal

Daniel F.O. Braga

LAETA, IDMEC, Instituto Superior Técnico,
Universidade de Lisboa
Portugal
<https://orcid.org/0000-0002-0587-3041>

Lucas F.M. da Silva

FEUP, University of Porto
Portugal
<https://orcid.org/0000-0003-3272-4591>

Pedro M.G.P. Moreira

INEGI, University of Porto
Portugal
<https://orcid.org/0000-0003-3272-4591>

Virgínia Infante

LAETA, IDMEC, Instituto Superior Técnico,
Universidade de Lisboa
Portugal
<https://orcid.org/0000-0003-0860-2404>

ABSTRACT: Even though friction stir welding (FSW) has been shown to produce high performing butt joints, stress concentration at the

weld edges in overlap FSW significantly reduces the performance of these joints. By combining FSW and adhesive bonding into a friction stir (FS) weld bonding, joint mechanical performance is greatly improved. Quasistatic and fatigue strength of the proposed FS weld-bonding joints was assessed and benchmarked against overlap FSW and adhesive bonding. The characterization of the structural adhesive is also presented, including differential scanning calorimetry (DSC) and thermogravimetric analysis (TGA), as well as mechanical characterization with curing temperature. A small process parameter study was made to select proper FSW parameters for AA6082-T6 overlap FSW and FS weld-bonded joints. FS weld bonding achieved a significant increase in quasistatic and fatigue strength when compared with overlap FSW, with 79.9% of the fatigue strength of adhesive-bonded joints at 10^6 cycles, whereas FSW had 41.6%.

KEYWORDS: Adhesive joints, fatigue, friction stir welding, welding.

1 | INTRODUCTION

Various drivers have pushed for the development and implementation of new joining processes in lightweight metal structures. One technology that has shown significant potential is friction stir welding (FSW) given the solid-state nature of the joining process. However, when welding large shell structures such as aeronautical fuselage panels, gaps may arise between the abutting faces to join leading to significant degradation of the joint mechanical

properties when butt welding. A study on the effect of gaps in mm thick aluminium alloy AA5083-H111 butt joints showed that gaps over 0.5 mm caused significant joint efficiency reduction.¹ To mitigate this issue, precise edge milling and appropriate clamping conditions are required. This is however very challenging for very long welds and the clamping conditions affects distortion levels and residual stress. The effect of clamping forces on residual stress, distortion and generate gaps was studied on AA2198-T851 FSW, making use of a specially made clamping system capable of measuring both the axial clamping loads, as well as horizontal clamping loads.² It was found that even welds that initially had 0-mm gap when welded with low clamping forces resulted in a measurable gap at the end of the weld. Higher clamping forces not only allowed to maintain the intended gap but also resulted in lower distortion and residual stress. The presence of gaps is especially concerning in the case of load control robotic FSW. Defects such as wormholes were also found to appear even in gaps lower than 0.5 mm, but their effect on hardness or mechanical performance was only verified at gaps above this value for 3.18-mm AA6061-T6 friction stir (FS) welds.³

Overlap FSW can overcome this limitation, but the edge of the weld in the advancing side forms a hook like defect, which diminishes the joint strength.^{4,5} Overlap FSW of 2-mm AA6082-T6 was found to achieve only a joint efficiency (joint ultimate load compared to base material ultimate tensile strength) of about 55% in quasistatic loading and 20–30% fatigue strength at 10^5 cycles.⁶ To improve strength in this joint configuration, it has been proposed to use multiple pass welding.⁵ By employing this method, the out-of-plane bending and peel load at these unwelded tips are reduced. This method, however, comes with disadvantages of its own. To accommodate the shoulder diameter and clamping, the overlaps must be larger, diminishing the weight savings gains. Lead time is also increased, along with tool wear, making the process less economically viable. Another way of improving the strength of overlap FSW joints is by combining it with another joining method such as adhesive bonding, resulting in FS weld bonding. This way the adhesive layer at the edges increases effective overlap and reduces peel stress at the weld edges. This method was used in magnesium-to-aluminium FS spot welded joints, resulting in increased quasistatic and fatigue strength.⁷ Similarly, this method was proposed for continuous overlap joints of AA2024-T3, resulting in improved quasistatic and fatigue strength.⁸ Lertora et al. studied FS weld bonding in weld-through and flow-in configuration of AA6082 aluminium alloy showing that the latter improved joint strength and joint fatigue life.⁹

This study covers hybrid overlap FSW and adhesive bonding (FS weld bonding) of an Al-Mg-Si alloy (AA6082-T6), which is a common multipurpose alloy. Characterization of the adhesive used in the study is first presented, including the effect of curing temperature in mechanical performance. This is relevant given that the adhesive in FS weld-bonded joints will not cure all at the same temperature. The degradation temperature is also measured through thermogravimetric analysis (TGA), to assess if it is below temperatures achieved during welding. FSW process parameters for FSW and FS weld-bonded joints were then

studied to find a set that results in sound quality joints. Finally, the joints were subjected to cyclic loading at $R = 0.1$ to assess the fatigue performance.

2 | EXPERIMENTAL DETAILS

2.1 Adhesive characterization

When joining large components as in the case of longitudinal fuselage joints, it may not be feasible to control curing temperature evenly, and as such, an adhesive capable of both curing at room temperature and elevated temperature is desirable. During FSW of FS weldbonded joints, the uncured adhesive will be subjected to an elevated temperature, which may locally accelerate the curing process. To assess the curing process of the chosen adhesive (Araldite 420 A/B), differential scanning calorimetry (DSC) was used. DSC analysis was performed on a Netzsch® DSC 200 F3 equipment on specimens with a mass of ≈ 50 mg, at a constant heating rate of 20 K min^{-1} from 21°C to 320°C in an atmosphere of constant flow of 20 ml min^{-1} of N_2 . Tensile mechanical properties of the adhesive were assessed through bulk tensile testing at 1-mm min^{-1} crosshead speed in an Instron testing machine. The bulk tensile specimens were made with four different curing conditions: room temperature for 7 days, 120°C for 1 h as indicated in the adhesive data sheet, 165°C and 200°C for 30 min. After curing, specimens were milled according to ASTM D638 standard.

As during the welding process, the adhesive will be subjected to high temperatures, having an adhesive with a high degradation temperature is important. TGA of the uncured epoxy adhesive was made on a Netzsch® Tg209 F3 Tarsus at 20 K min^{-1} from 21°C to 600°C , allowing the determination of the degradation temperature of the adhesive.

To determine shear strength and shear modulus, thick adherend shear test (TAST) and Poisson ratio measurement were made according to ASTM D5656-10 and ASTM E132-17, respectively. Two curing conditions were assessed: room temperature for 1 week and 120°C for 1 h.

Given the complex loading case of single lap joints, with combination of peel and shear load on the adhesive, fracture toughness of the adhesive in mode I and II was assessed through double cantilever beam (DCB) specimens and end notch flexure (ENF) specimens. In both tests, specimens had the same dimensions, being composed of two steel beams with $320 \times 25 \times 12.7$ mm bonded by a layer of 0.2-mm-thick adhesive, differing only on the loading method. Specimens used for fracture toughness assessment were cured at room temperature for 7 days, and as an approximation, it was assumed that fracture toughness remained unchanged with curing condition. However, it may be expected that some fracture toughness is lost with increasing curing temperature, and as such, the real values may be lower.¹⁰ DCB specimens were loaded at 1-mm min^{-1} crosshead speed and the resulting load versus displacement curves were used to plot the corresponding R curves

using the compliance-based beam method (CBBM).¹¹ Following the DCB fracture tests, a 3D numerical model of the test was created in Abaqus, using the same dimensions, and loading conditions. The adhesive was modelled using cohesive zone modelling (CZM), with a single layer of 0.2-mm-thick COH3D8 elements. The quadratic nominal stress criterion was used as damage initiation criteria, and the experimentally measured mechanical properties were set as input. A trapezoidal cohesive law was used to model the adhesive, given the high strength and toughness measured. The resulting *R* curve and load versus displacement curve were compared with the experimental DCB curves as a verification of the measured fracture toughness or as an inverse parameter identification method. For mode II, ENF testing was performed at 0.2-mm min⁻¹ crosshead speed. Similarly, to the DCB tests in mode I, the ENF tests were also analysed through CBBM method but in this case for mode II loading.¹² Like in the case of mode I, a 3D numerical model of the ENF test was made. The model is similar in all aspects to the DCB model, except for the loading conditions, where rigid shells were used to model the rollers of the 3-point bending apparatus.

2.2 Aluminium base material and welding condition

The alloy used in this study was the AA6082-T6. The chemical composition is shown in Table 1 and the mechanical properties in Table 2.

AA6082-T6 300 × 150 × 2-mm plates were welded with a 40-mm overlap. All welding procedures were performed on a dedicated FSW ESAB® LEGIO 3UL numerical control machine. In FS weld bonding, the welding procedure was done with the adhesive in a noncured state and right after adhesive lay-up and joint closing. Calibrated metal strips with 0.2-mm thickness were strategically positioned in-between the shim plates to ensure a more uniform adhesive thickness (0.2 mm).

Prior to bonding, surfaces were degreased and sanded. In the case of adhesive-bonded joints, phosphoric acid anodization (PAA) according to ASTM D3933-98(2017) standard was used, whereas FS weld-bonded joints were subjected to chemical treatment with 3M® AC-130, which is a sol-gel anodization replacement normally intended for aeronautical repair.¹⁴

The FSW tool used had 5-mm-diameter cylindrical threaded pin with 3-mm length and 16-mm-diameter grooved shoulder. The FSW process parameters used are listed in Table 3. These were chosen based on literature review and past experience. Various levels of downward force were tested to assess its effect on joint performance and maximize joint strength.

2.3 Joints characterization

All joint configurations were tensile tested with three specimens each. Tensile testing was done in an Instron® 3369 machine with a 50-kN load cell at 1-mm min⁻¹ crosshead speed. Three specimens of each joint configuration were tested. Joint efficiency was

calculated dividing maximum axial load by the substrate cross-section outside of the overlap as in previous works.^{5,13}

Optical microscopy analysis of the joints cross-section was performed on an Olympus CK40M microscope after sanding, polishing, and etching with Keller's reagent. Microhardness measurement was then made in the same specimens on a Shimadzu HMV-2, applying a load of 0.2 HV. Measurements were made along three lines in the cross-section, at 0.5 mm from the top surface, 0.8 mm from the root surface and 1.6 mm from the root surface. The spacing between measurements along each line was 0.3 mm.

An assessment of the fatigue strength of FSW, FS weld-bonded and adhesive-bonded joints was then made under constant amplitude, at a load ratio of $R = 0.1$ in an Instron 8874 machine with a 10-kN load cell, at 8 Hz. For this study, both FSW and FS weld-bonded joints were made using 450-kgf downward force during FSW. For each joint configuration, four load levels were used with three specimens per load level. The probabilistic $S-N$ curves were calculated using ProFatigue software.

Mn	Fe	Mg	Si	Cu	Zn	Ti	Cr	Others (total)	Al
0.40	0.50	0.60	0.70	0.10	0.20	0.10	0.25	0.10	Balance
1.00		1.20	1.30						

TABLE 1 Chemical composition of AA6082-T6 (% mass)²⁶

Density (kg m ⁻³)	Vickers hardness	Ultimate tensile strength (MPa)	Yield tensile strength (MPa)	Elongation at break (%)
2700	95	290	250	10

TABLE 2 AA6082-T6 mechanical properties²⁶

Parameter	Parameter
FSW control	Vertical force
Rotation direction	Clockwise (CW)
Plunge speed	0.1 mm s ⁻¹
Dwell time	6 s
Tilt angle	0°
Welding speed	200 mm min ⁻¹
Rotational speed	1000 rpm
Downward force	400/425/450/500/550 kgf

Abbreviation: FSW, friction stir welding.

TABLE 3 FSW process parameters

3 | RESULTS AND DISCUSSION

3.1 Adhesive characterization

A representative curve of the DSC analysis is shown in Figure 1. According to it, most of the curing process occurs at elevated temperatures, with peak curing at $\approx 120^\circ\text{C}$, even though the adhesive has the capacity to cure at room temperature as indicated by the datasheet. An endothermic event is also observed at about 200°C in all samples tested, which is believed to be evaporation of water, after exceeding the sealing limit of the sample container (water vapour pressure at 200°C is $\approx 15\text{ Atm}$).

From the DSC analysis, it may be inferred that full curing does not occur at room temperature, leading the adhesive to have different mechanical behaviour with different curing conditions. Tensile testing of the bulk adhesive further confirms this assumption. The resulting stress versus strain curves for the four curing conditions are presented in Figure 2.

An increase in ultimate strength was observed with increasing curing temperature, accompanied by a reduction in elongation at break. This behaviour may be due to increased cross-linking of the polymeric chains with increasing cure temperature. The change is more significantly from room temperature to 120°C cure condition than from 120°C to further higher temperatures. This is consistent with the DSC analysis results were most of the curing was shown to happen around 120°C .

The TGA resulted in the TG curves presented in Figure 3, where the onset of degradation was found to be at $357.3^{+2}\text{ }^\circ\text{C}$. During FS weld bonding, temperatures in the adhesive at 16 mm from the weld bead centre were reported to be between 200°C and 250°C , which when combined with the microscopic analysis of the cross section leads to conclude that no significant degradation will occur during the welding procedure.¹⁵

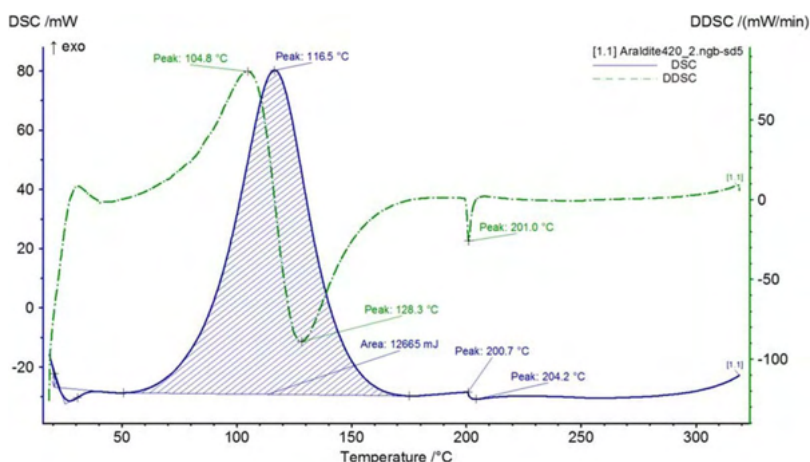


FIGURE 1 Representative curve of differential scanning calorimetry (DSC) analysis of the uncured epoxy adhesive [Colour figure can be viewed at wileyonlinelibrary.com]

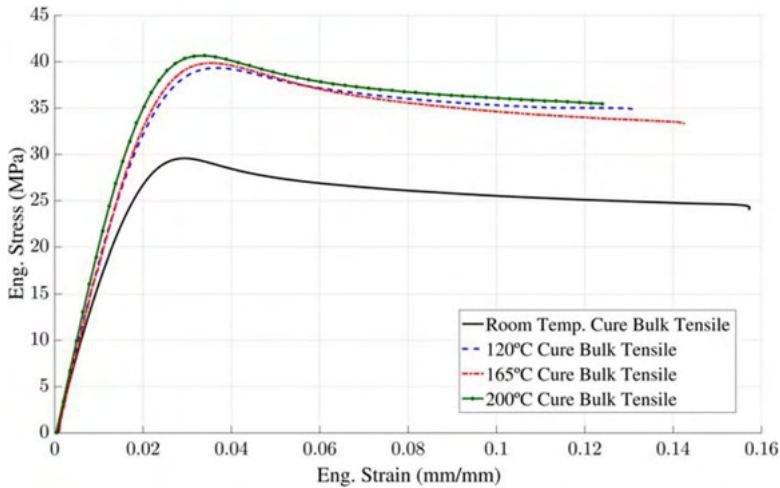


FIGURE 2 Representative Araldite 420 stress versus strain curves with curing temperature [Colour figure can be viewed at wileyonlinelibrary.com]

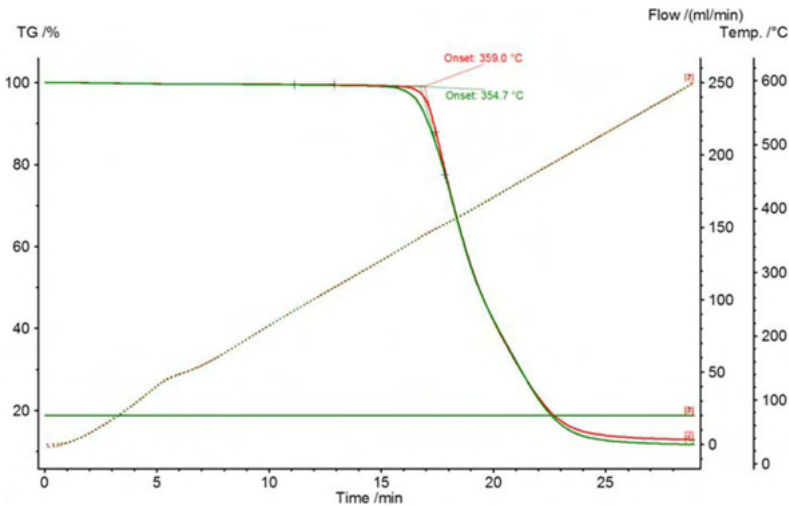


FIGURE 3 Thermogravimetric analysis (TGA) of uncured epoxy adhesive [Colour figure can be viewed at wileyonlinelibrary.com]

Figure 4 presents a representative R curve regarding the mode I DCB fracture tests. The critical fracture toughness in mode I measured was $3 \pm 0.37 \text{ N mm}^{-1}$. This value is relatively high compared with other structural adhesives^{16,17} and continuous fibre reinforced composites,¹⁸ showing that the chosen epoxy has high fracture resistance.

From the 3D numerical model of the DCB test, good agreement was achieved with the experimental results. Experimental results were obtained when performing the mode I fracture testing with the DCB specimens, recording the load directly from the load cell and the displacement with the testing machine LVDT. The load versus displacement curves showing this good agreement are shown in Figure 5.

A representative R curve obtained in the ENF tests is presented in Figure 6. The critical fracture toughness measured in mode II was $11.6 \pm 0.3 \text{ N mm}^{-1}$. However, the maximum bending load was relatively high, which may have induced local plasticization, and as such, the measured mode II fracture toughness may be artificially high. A parametric study was then used to find an adequate adhesive fracture toughness in mode II, by keeping constant all other material parameters and comparing numeric and experimental loads versus displacement curves.

The Abaqus model showed that indeed 11.6 N mm^{-1} was an overestimation of the critical fracture toughness in mode II and by an iterative process that 9 N mm^{-1} resulted in better agreement with the experimental load versus displacement curves as shown in Figure 7. This value is still relatively high fracture strength when compared with adhesives reported in the literature.^{19,20} There was a small difference in terms of stiffness between numerical model and experimental data, which was consistent in all numeric runs and is probably due to the experimental loading configuration. As the ENF test is performed in 3-point bending, the machine is operated in compression and the displacement values measured include all the slack within the system, whereas in the numerical model, no such limitations exist.

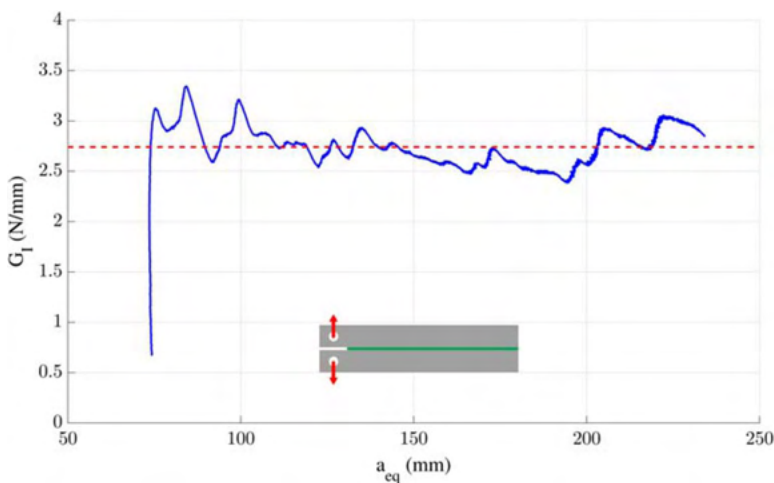
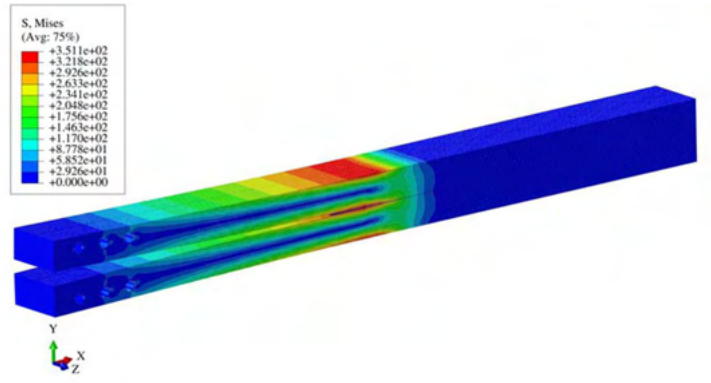
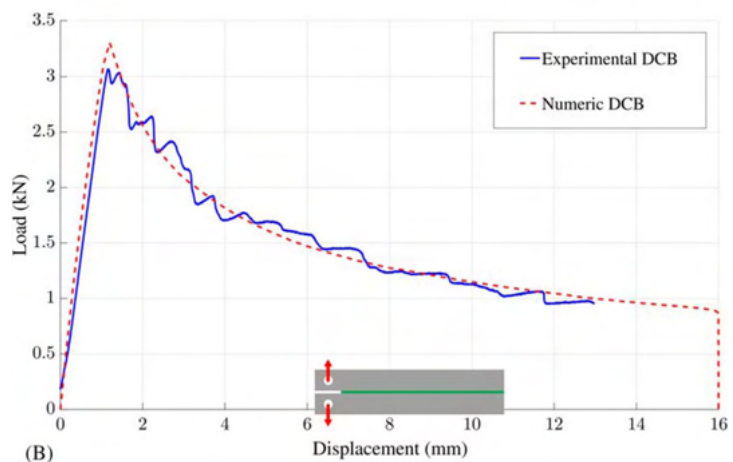


FIGURE 4 Representative adhesive R curve for mode I [Colour figure can be viewed at wileyonlinelibrary.com]



(A)



(B)

FIGURE 5 (A) von Mises stress in 3D double cantilever beam (DCB) Abaqus model at 5-mm displacement and (B) load displacement curve comparison between numeric and experimental [Colour figure can be viewed at wileyonlinelibrary.com]

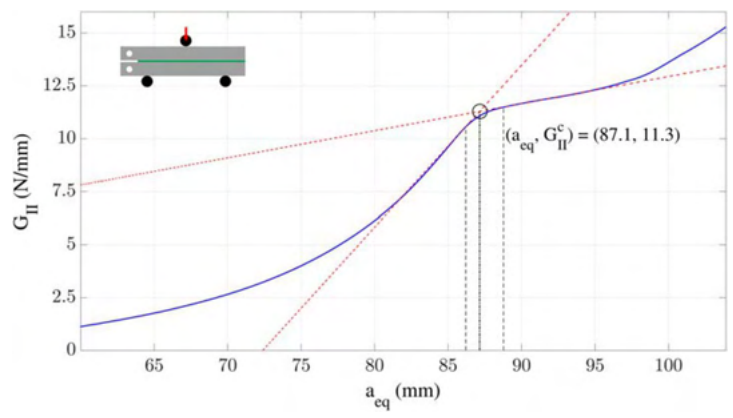


FIGURE 6 Representative adhesive R curve for mode II [Colour figure can be viewed at wileyonlinelibrary.com]

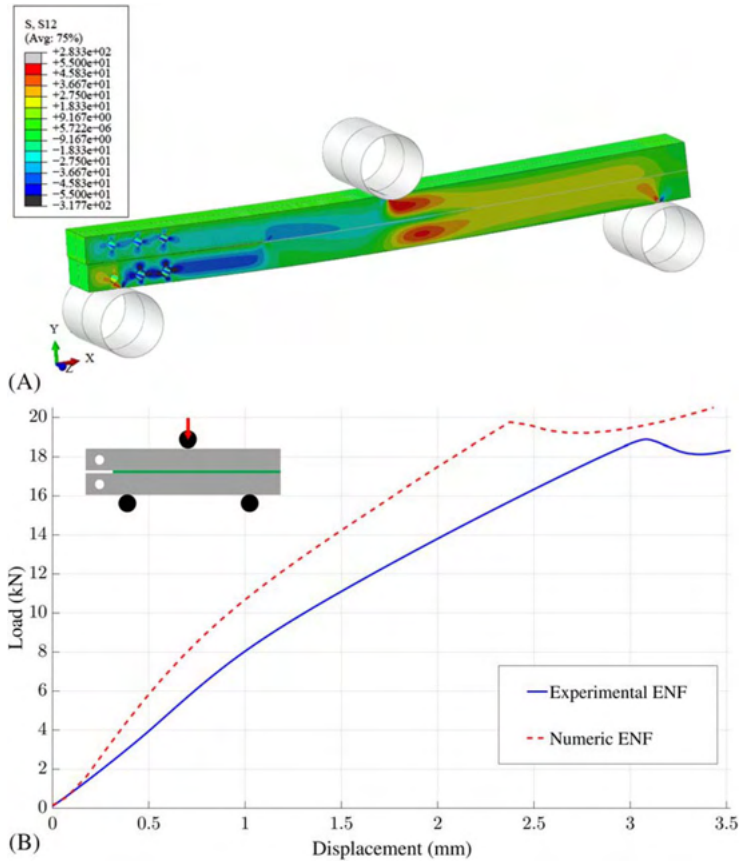


FIGURE 7 (A) Shear stress in 3D end notch flexure (ENF) Abaqus model at the onset of damage and (B) displacement curve comparison between numeric and experimental [Colour figure can be viewed at wileyonlinelibrary.com]

The numerical modelling highlights the high mechanical strength and toughness of the adhesive chosen and serves as a tool for further modelling of more complex joint configurations. The experimental characterization of the adhesive is summarized in Table 4, with the mechanical properties of the adhesive for two curing conditions.

3.2 Joints mechanical performance

After quasistatic testing of the FSW and FS weldbonded joints manufactured with varying process parameters, an analysis was made of the effect of these process parameters in the mechanical performance. Figure 8 compares the joint efficiency of the joint configurations tested.

When comparing FS weld-bonded joints to FSW, it was possible to observe an improvement of 20–30% in most cases. When comparing the best performing FSW and FS weld-bonded joints, an improvement of more than 50% was found which is higher than reported in the literature for weld-though FS weld-bonded joints.⁹ It was possible to

observe that for FSW joints, the increase in downward force results in an increase of joint strength. This may be related with higher thermal input, which leads to further softening of the work-piece. The further softening of the workpiece may result in better mixing and as such diminishing the hook defect size, as presented in Maciel et al.²¹ For FS weld-bonded joints, the trend is not as clear as in FSW joints, as it increases from 400 to 450 kgf but diminishes from then on. The reasoning for this decrease may be due to high downward force leading to excessive adhesive thinning or possibly the higher temperature may lead to degradation of the surface to bond and/or the adhesive. As such, for the metallographic analysis and fatigue study, joints will not be fabricated with downward forces higher than 450 kgf. FS weld-bonded joints also showed higher dispersion in terms of joint strength than FSW, which may be due to variations in surface treatment, as the joint strength is very sensitive to the bonding strength. Figure 9 compares the highest strength FSW and FS weld-bonded joints with adhesivebonded joints.

In Figure 10, the microhardness profile and joint cross-section of the best performing FS weld-bonded joint are presented. It is possible to observe that the hook defect formed by the upward flow of material generated in the advancing side is present. The size and shape of this defect is critical to overlap FSW joint strength.²¹ Along with the hook defect, it is also observable a cold lap defect on the retreating side of the weld, which is a result of the initial upward flow under shearing effect of the pin followed by a downward flow in order to fill the space at the bottom of the pin. However, these defects become less critical in FS weld-bonded joints when compared with FSW as the adhesive increases the effective joined overlap and reduces loading the weld edges.

A loss of hardness is presented in the microhardness profile, which is due to the loss of T6 condition from the temperatures reached during welding. Heat is generated due to friction between the tool and workpiece, which leads to higher temperatures in this contact surface,²² and as such, a wider cross-section of the joint has lower hardness at the top. An increase in hardness, although not to the level of base material, is observed in the centre of the weld, especially on the top measurement (forming a typical W shape of heat-treated aluminium alloys FSW) due to the dynamic recrystallization that occurs in the stir zone.²³

After the joints metallographic and quasistatic mechanical performance characterization, fatigue testing was conducted under constant amplitude loading. Figure 11 shows the resulting *S-N* curves including 50% and 5% probability of failure calculated using ProFatigue soft-ware.²⁴ A *S-N* curve regarding the AA6082-T6 base material reported in a previous work²⁵ was also included.

Cure condition	E (GPa)	G (MPa)	σ (MPa)	τ (MPa)	G^c_{\perp} (N mm ⁻¹)	G^c_{\parallel} (N mm ⁻¹)
Room temperature for 7+ days	1.57	600	30	22.5	3	9 ^a
120°C for 1 h	1.73	665	40	28	3 ^b	9 ^{a,b}

^aConsidering the value obtained through numerical modelling of the experimental procedure.

^bConsidering the same fracture toughness than in room temperature.

TABLE 4 Araldite 420 mechanical properties

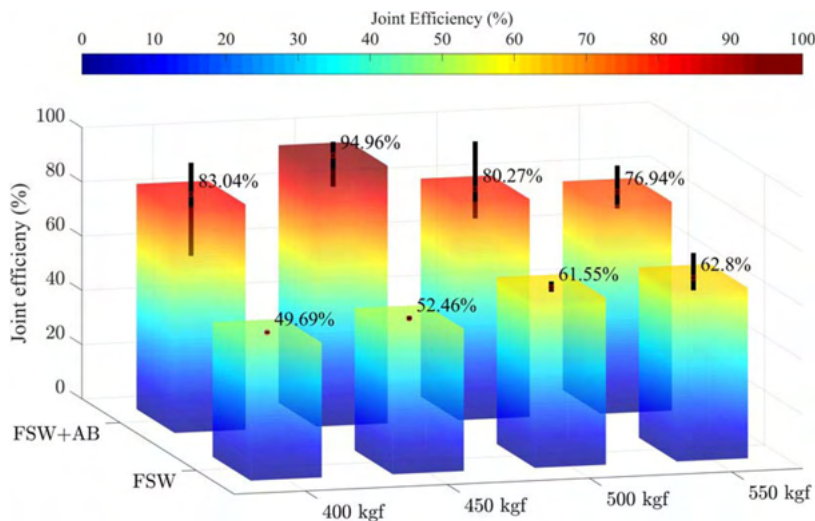


FIGURE 8 Joint efficiency of friction stir welding (FSW) and friction stir (FS) weld-bonded joints with differing downward force in the FSW tool during joining [Colour figure can be viewed at wileyonlinelibrary.com]

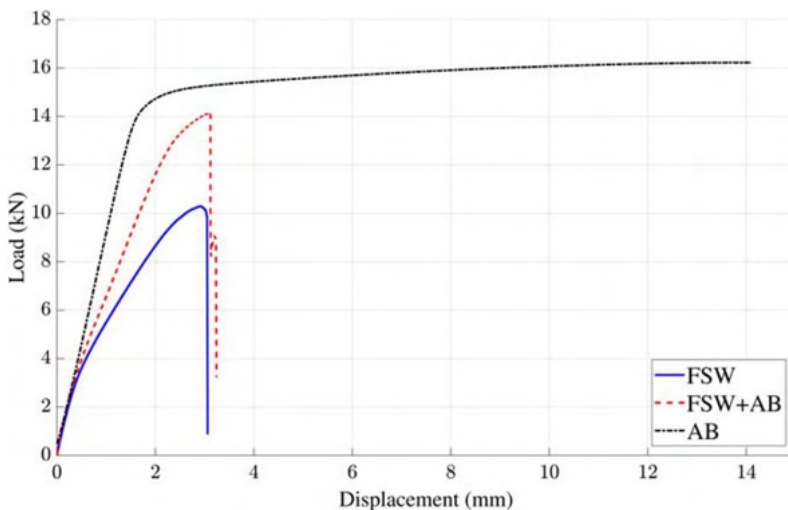


FIGURE 9 Stress versus displacement of highest strength friction stir welding (FSW) and friction stir (FS) weld-bonded joints along the adhesive bonded [Colour figure can be viewed at wileyonlinelibrary.com]

FSW joints showed lower fatigue strength than adhesive and FS weld-bonded joints as it would be expected given the lower quasistatic strength. The FS weld bonded showed similar fatigue strength to adhesive-bonded joints. Adhesive-bonded joints still had the highest fatigue strength of all joints tested, which is to be expected given the more continuous stress distribution in these joints. At 10^6 cycles, adhesive-bonded joints have a 50% probability of failure at 56.4 MPa, whereas FS weld bonding and FSW at the same number of cycles, the 50% probability of failure is achieved at 45.1 (79.9% of adhesive-bonded joints) and 23.5 MPa (41.6% of adhesive-bonded joints). The failure modes were consistent with the quasistatic ones, with the adhesive failing in adhesive/cohesive way, the FSW failing through the hook defect and the FS weld-bonded ones failing through the adhesive layer followed by cracking through the hook.

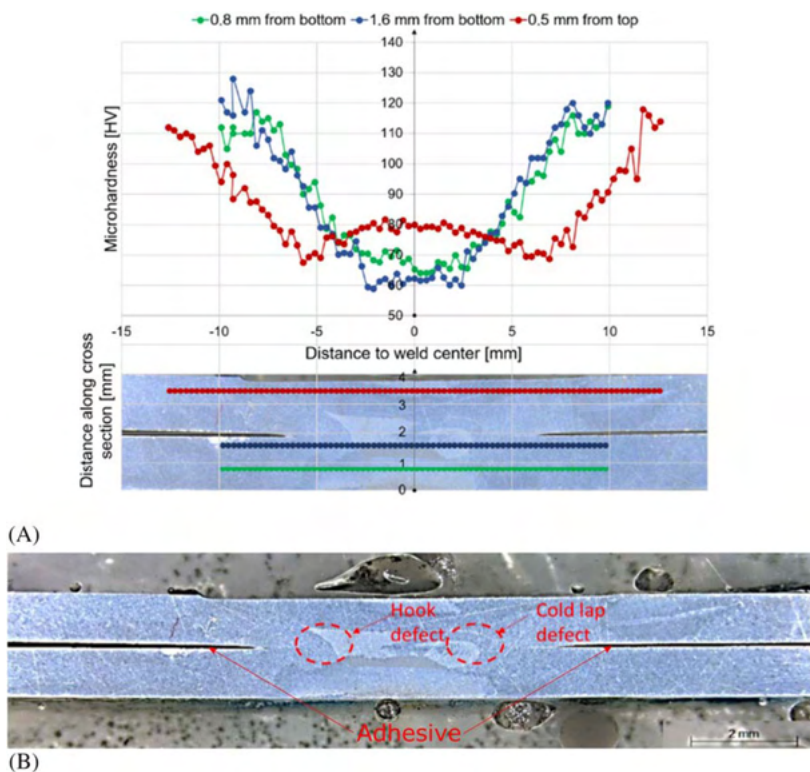


FIGURE 10 (A) Microhardness profile and (B) joint cross-section of friction stir (FS) weld-bonded joint with 450 kgf [Colour figure can be viewed at wileyonlinelibrary.com]

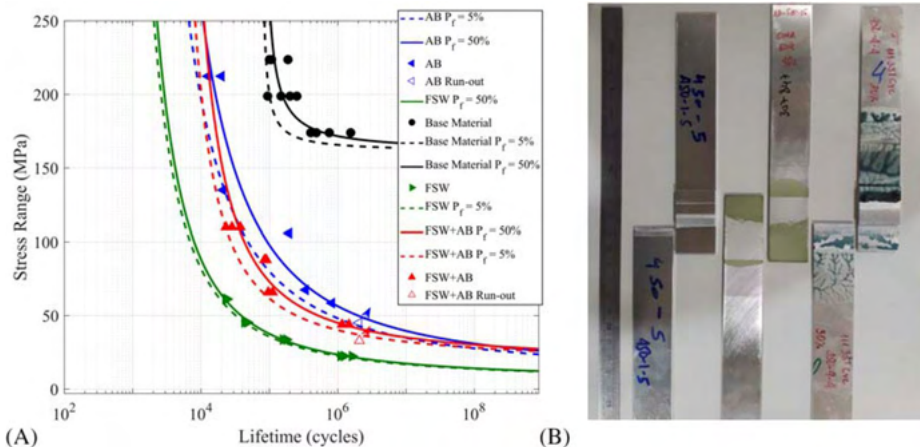


FIGURE 11 (A) p - S - N curves of the three joint type and (b) failure modes [Colour figure can be viewed at wileyonlinelibrary.com]

4 I CONCLUDING REMARKS

The combination of FSW and adhesive bonding into FS weld bonding was studied regarding quasistatic and fatigue performance. In order to benchmark the process, it was compared against overlap FSW and adhesive bonding.

The epoxy adhesive used was characterized taking into consideration the curing temperature, showing that even though it cures at room temperature, higher temperature curing will increase strength while reducing ductility. Degradation temperature was also found to be above reported temperatures incurred during the welding procedure.

In the joints quasistatic testing, overlap FSW showed lower strength and ductility than FS weld-bonding joints. Downward force during welding showed a significant effect in strength and ductility of FSW joints, with both increasing up to 550 kgf. The same trend was not observed in the FS weld-bonded joints, with the highest strength and ductility achieved at 450 kgf, with a joint efficiency of 94.96%. In FS weld-bonded joints, the critical weld edges were kept close by the adhesive, leading to increase mechanical performance. As such, adhesive strength and the quality of the surface treatment are more significant to joint strength than downward force during welding. Adhesive-bonded joints showed the highest strength and ductility given the relatively large overlap.

In cyclic loading at $R = 0.1$, similar trends to the quasistatic loading were observed. Adhesive bonding achieved the highest fatigue strength followed by FS weld bonding and FSW showed significantly lower fatigue strength (41.6% strength of adhesive-bonded joints at 10⁶ cycles). The hook defect serves as a fatigue crack initiation location and leads to the failure of FSW joints. Adhesive joints fail in an adhesive/cohesive manner, whereas FS weld bonding fail through the adhesive immediately followed by cracking through the hook defect.

ACKNOWLEDGEMENTS

This work was supported by FCT, through IDMEC, under LAETA, project UIDB/50022/2020. Funding provided from NORTE-01-0145-FEDER-000022 SciTech— Science and Technology for Competitive and Sustainable Industries is acknowledged. The authors acknowledge the funding provided by Fundação para Ciência e a Tecnologia (FCT) project PTDC/EME-EME/29340/ 2017— DisFri.

AUTHOR CONTRIBUTIONS

Ricardo Maciel and Tiago Bento produced and tested the FSW and FS weld-bonding joints. Daniel F.O. Braga produced and tested the adhesive joints, performed the adhesive characterization tests, was involved in the conception and design of the study and wrote the manuscript. Lucas F.M. da Silva was involved in the conception and design of the study, analysed and interpreted data regarding adhesive characterization and testing and revised the manuscript. Pedro M.G.P. Moreira was involved in the conception and design of the study, analysed and interpreted data regarding FSW and FS weld-bonding joints and revised the manuscript. Virginia Infante was involved in the conception and design of the study, analysed and interpreted data regarding fatigue testing and revised the manuscript.

AUTHORSHIP STATEMENT

All persons who meet authorship criteria are listed as authors, and all authors certify that they have participated sufficiently in the work to take public responsibility for the content, including participation in the concept, design, analysis, writing or revision of the manuscript. Furthermore, each author certifies that this material or similar material has not been and will not be submitted to or published in any other publication before its appearance in the *Fatigue & Fracture of Engineering Materials & Structures* journal.

FUNDING INFORMATION

SciTech— Science and Technology for Competitive and Sustainable Industries, Grant/ Award Number: NORTE-01-0145-FEDER-000022; Fundação para Ciência e a Tecnologia (FCT), Grant/ Award Numbers: PTDC/EME- EME/29340/2017, UIDB/50022/2020

REFERENCES

1. Shultz EF, Cole EG, Smith CB, Zinn MR, Ferrier NJ, Pfefferkorn FE. Effect of compliance and travel angle on friction stir welding with gaps. *J Manuf Sci Eng*. 2010;132(4): 041010–041019.
2. Richter-Trummer V, Suzano E, Beltrão M, Roos A, dos Santos JF, de Castro PMST. Influence of the FSW clamping force on the final distortion and residual stress field. *Mater Sci Eng A*. 2012;538:81-88.

3. Wanjara P, Monsarrat B, Larose S. Gap tolerance allowance and robotic operational window for friction stir butt welding of AA6061. *J Mater Process Technol.* 2013;213(4):631-640.
4. Fersini D, Pironi A. Fatigue behaviour of Al2024-T3 friction stir welded lap joints. *Eng Fract Mech.* 2007;74(4):468-480.
5. Papadopoulos M, Tavares S, Pacchione M, Pantelakis S. Mechanical behaviour of AA 2024 friction stir overlap welds. *Int J Struct Integr.* 2013;4(1):108-120.
6. Ericsson M, Jin L-Z, Sandström R. Fatigue properties of friction stir overlap welds. *Int J Fatigue.* 2007;29(1):57-68.
7. Chowdhury SH, Chen DL, Bhole SD, Cao X, Wanjara P. Lap shear strength and fatigue behavior of friction stir spot welded dissimilar magnesium-to-aluminum joints with adhesive. *Mater Sci Eng A.* 2013;562:53-60.
8. Braga DFO, Maciel R, Bergmann L, et al. Fatigue performance of hybrid overlap friction stir welding and adhesive bonding of an Al-Mg-Cu alloy. *Fatigue Fract Eng Mater Struct.* 2019;42(6): 1262-1270.
9. Lertora E, Mandolino C, Pizzorni M, Gambaro C. Influence of adhesive in FSW: investigation on fatigue behavior of welded, weld-bonded, and adhesive-bonded joints in aluminum AA 6082 T6. *Materials.* 2019;12(8):1242–1253.
10. Incerti D, Wang T, Carolan D, Fergusson A. Curing rate effects on the toughness of epoxy polymers. *Polymer.* 2018;159: 116-123.
11. de Moura MFSF, Dourado N. Mode I fracture characterization of wood using the TDCB test. *Theor Appl Fract Mech.* 2018;94: 40-45.
12. de Moura MFSF, Silva MAL, de Moraes AB, Morais JLL. Equivalent crack based mode II fracture characterization of wood. *Eng Fract Mech.* 2006;73(8):978-993.
13. Infante V, Braga DFO, Duarte F, Moreira PMG, de Freitas M, de Castro PMST. Study of the fatigue behaviour of dissimilar aluminium joints produced by friction stir welding. *International Journal of Fatigue.* 2016;82:310-316.
14. McCray D, Smith J, Mazza J, Storage K. Evaluation of adhesive bond primers for repair bonding of aluminum. Air Force Research Lab Wright-Patterson AFB OH Materials and Manufacturing; 2011.
15. Braga DFO. *Innovative structural joining for lightweight design.* Faculty of Engineering of the University of Porto. 2018.
16. Banea MD, Silva LD, Campilho RDSG. Effect of temperature on tensile strength and mode I fracture toughness of a high temperature epoxy adhesive. *J Adhes Sci Technol.* 2012;26(7): 939-953.
17. de Moura MFSF, Campilho RDSG, Gonçalves JPM. Crack equivalent concept applied to the fracture characterization of bonded joints under pure mode I loading. *Compos Sci Tech.* 2008;68(10):2224-2230.
18. Machado JJM, Marques EAS, Campilho R, da Silva LFM. Mode I fracture toughness of CFRP as a function of temperature and strain rate. *J Compos Mater.* 2016;51(23):3315-3326.

19. de Moura MFSF, Campilho RDSG, Gonçalves JPM. Pure mode II fracture characterization of composite bonded joints. *Int J Solid Struct.* 2009;46(6):1589-1595.
20. Azevedo JCS, Campilho RDSG, da Silva FJG, Faneco TMS, Lopes RM. Cohesive law estimation of adhesive joints in mode II condition. *Theor Appl Fract Mech.* 2015;80:143-154.
21. Maciel RL, Infante V, Braga D, Moreira P, Bento T, da Silva L. Development of hybrid friction stir welding and adhesive bonding single lap joints in aluminium alloys. *Fratt Integr Strutt.* 2019;13(48):269-285.
22. Aziz SB, Dewan MW, Huggett DJ, Wahab MA, Okeil AM, Warren LT. Impact of friction stir welding (FSW) process parameters on thermal modeling and heat generation of aluminium alloy joints. *Acta Metall Sin (English Letters).* 2016;29(9): 869-883.
23. Costa MI, Rodrigues DM, Leitão C. Analysis of AA 6082-T6 welds strength mismatch: stress versus hardness relationships. *Int J Adv Manuf Tech.* 2015;79(5):719-727.
24. Fernández-Canteli A, Przybilla C, Nogal M, Aenlle ML, Castillo E. ProFatigue: a software program for probabilistic assessment of experimental fatigue data sets. *Proc Eng.* 2014;74: 236-241.
25. Moreira PMGP, Richter-Trummer V, de Castro PMST. Fatigue behaviour of FS, LB and MIG welds of AA6061-T6 and AA6082-T6. Paper presented at: Multiscale Fatigue Crack Initiation and Propagation of Engineering Materials: Structural Integrity and Microstructural Worthiness; 2008; Dordrecht.
26. Matweb. <http://www.matweb.com>; 2020.

ÍNDICE REMISSIVO

A

Ácido polilático 105, 106
Adhesive joints 111, 124, 125, 127
Análise de vibração 62
Arranjo físico posicional 128, 129, 130, 131
Atraso de ignição 62, 63, 64, 65, 66, 67

B

Bateria eletrônica 149, 150, 151, 152, 155, 157
Biomassa 1, 2, 3, 5, 6, 7, 8, 9, 10, 11, 12, 15, 19

C

Cianobactérias 13, 14, 15, 16, 17, 19
Concreto 68, 69, 73, 82, 83, 84, 85, 86, 88, 89, 90, 91, 92, 93, 94, 96, 97, 99, 100, 103, 104
Construção civil 68, 69, 73, 78, 80, 81, 82, 104

D

Desenho geométrico 158, 159, 160, 162, 163, 172
Distribuição de água 34, 35, 36, 37, 39, 40, 42, 43, 47, 48, 49, 50

E

Economia 34, 59, 78, 163, 180, 183, 185, 188
Educação 146, 157, 158, 159, 160, 161, 162, 171, 172, 185, 187
Efluente sintético 13, 16
Empreendedorismo 185, 186, 187, 188, 189
Estruturas mistas 82, 83, 84, 86, 88, 94, 103, 104

F

Fluido 51, 53, 55, 60
Friction stir welding 111, 115, 122, 126, 127

G

Gesso 68, 69, 70, 71, 72, 73, 74, 75, 76, 77, 78, 79, 80, 81

I

Impressora 3D 105, 106, 108, 110

L

Logística reversa 21, 22, 23, 26, 30, 31, 32

M

Macromedição 36

Madeira 6, 8, 69, 82, 83, 84, 85, 86, 87, 88, 89, 90, 91, 92, 93, 94, 95, 96, 97, 98, 99, 100, 101, 102, 103, 104

Matriz energética 1, 2, 3, 4, 5, 6, 8, 10

Micromedição 36

Música 149, 150, 151, 157

O

Otimização 128, 143

P

Planejamento estratégico 2, 185

Plano de negócio 179

Proteção 4, 72, 77, 85, 174, 175, 176

R

Reaproveitamento 78, 80

Recuperação avançada de petróleo 51, 52

Reservatório 18, 51, 52, 55

S

Segurança da informação 173, 174, 175, 176, 181, 182, 183, 184

Segurança estrutural 82

Sensor piezoelétrico 62, 63, 64, 65, 66

Sistema de ligação 82, 83, 85, 86, 90, 92, 94, 101, 103

Sustentabilidade 11, 21, 22, 68, 78, 80

T

Tear modular 107, 110

Tecnologia 7, 19, 68, 69, 81, 105, 106, 110, 125, 149, 150, 151, 152, 158, 159, 160, 162, 164, 170, 171, 175, 176, 177, 182, 183, 184, 190

Tensoativo 51, 53

Toxicidade 13, 14, 15, 17, 106

Tratamento de efluente 13

www.atenaeditora.com.br



contato@atenaeditora.com.br



@atenaeditora



www.facebook.com/atenaeditora.com.br



ENGENHARIAS:

Criação e repasse de tecnologias 3



www.atenaeditora.com.br 

contato@atenaeditora.com.br 

@atenaeditora 

www.facebook.com/atenaeditora.com.br 

ENGENHARIAS:

Criação e repasse de tecnologias 3

